Bosonic Pair Production and Squeezing for Optical Phase Measurements in Long-Lived Dipoles Coupled to a Cavity

Bhuvanesh Sundar,[1,2] Diego Barberena,[1,2] Asier Piñeiro Orioli,[1,2] Anjun Chu,[1,2] James K. Thompson,[2] Ana Maria Rey,[1,2] and Robert J. Lewis-Swan[3,4]

[1]*Center for Theory of Quantum Matter, University of Colorado, Boulder, Colorado 80309, USA*
[2]*JILA, NIST, Department of Physics, University of Colorado, Boulder, Colorado 80309, USA*
[3]*Homer L. Dodge Department of Physics and Astronomy, The University of Oklahoma, Norman, Oklahoma 73019, USA*
[4]*Center for Quantum Research and Technology, The University of Oklahoma, Norman, Oklahoma 73019, USA*

(Received 30 April 2022; accepted 14 February 2023; published 15 March 2023)

We propose to simulate bosonic pair creation using large arrays of long-lived dipoles with multilevel internal structure coupled to an undriven optical cavity. Entanglement between the atoms, generated by the exchange of virtual photons through a common cavity mode, grows exponentially fast and is described by two-mode squeezing of effective bosonic quadratures. The mapping between an effective bosonic model and the natural spin description of the dipoles allows us to realize the analog of optical homodyne measurements via straightforward global rotations and population measurements of the electronic states, and we propose to exploit this for quantum-enhanced sensing of an optical phase (common and differential between two ensembles). We discuss a specific implementation based on Sr atoms and show that our sensing protocol is robust to sources of decoherence intrinsic to cavity platforms. Our proposal can open unique opportunities for next-generation optical atomic clocks.

DOI: 10.1103/PhysRevLett.130.113202

The generation of robust and scalable quantum squeezing on an optical transition has the potential to vastly improve optical frequency standards in state-of-the-art atomic clocks and significantly advance capabilities in a variety of fields ranging from gravimetry [1] to fundamental physics [2–9]. Despite this promise, experiments have not yet used squeezing to make any practical improvements to optical frequency standards in state-of-the-art clocks beyond proof-of-principle experiments [10,11], due to a variety of physical and technical challenges. As a result, the development and theoretical study of new proposals to generate scalable, robust entangled states that simultaneously minimize experimental complexity and respect technical constraints are a crucial task to make concrete progress in the field of quantum-enhanced metrology [1,12–19].

In this Letter, we introduce two-mode squeezing (TMS) of atoms in a cavity-QED platform as a feasible path to quantum-enhancement of state-of-the-art clocks. TMS is realized as the result of a process that produces entangled pairs of particles. Prior realizations of TMS in photonic systems generated entangled photons via, e.g., four-wave mixing (FWM) of optical fields in a nonlinear medium [20]. Complementary efforts in ultracold bosonic gases have used the intrinsic nonlinearity provided by contact interactions [12,21–26], including spinor Bose-Einstein condensates (BECs) [27–33], wherein spin-changing collisions between atoms of different internal spin states simulate pair production analogous to degenerate FWM of optical fields [34]. Experiments have also generated TMS via quantum non-demolition (QND) measurements of thermal gases [35–40]. However, these experiments have all been challenged by a variety of factors—short interaction times in photonics, finite detection efficiency in QND measurements, and complex spatial dynamics in spinor BECs that limits their scalability [41,42].

We propose to simulate a pair production process through light-mediated interactions between atoms confined in an undriven optical cavity and exploit it for quantum-enhanced metrology. Pairs of entangled excitations are generated by the exchange of virtual photons between a quartet of internal spin states coupled to a common, far-detuned cavity mode, in a process analogous to FWM. The pinning of the atoms in a deep optical lattice supported by the cavity, in combination with the global range of the effective interaction [43], avoids undesirable motional decoherence and can enable the study of large systems. The exploitation of light-mediated unitary exchange interactions realized by coupling an optical transition to an undriven cavity complements prior work involving Raman transitions [16,44], and avoids potential sources of technical noise introduced by driving the cavity with an external field, such as fluctuations in the drive intensity or detuning. Nevertheless, our proposal can in principle be extended to these systems.

TMS states are well known to have excess quantum fluctuations in the phase and amplitude quadratures of each bosonic mode, but suppressed fluctuations of combined quadratures of the two modes. We demonstrate that, despite the complexity of our underlying physical system, the generated quadrature squeezing can be readily accessed and exploited for quantum-enhanced sensing by a sequence of rotations and population measurements that are straightforward to implement and shown to be equivalent to a standard Ramsey sequence. Moreover, engineering TMS on two distinct long-lived optical transitions lets us design protocols to sense both differential and sum phases imprinted on the atoms. This is a distinct advantage of our scheme compared to, e.g., atomic homodyne techniques that have been developed in spinor BECs but require simultaneous mixing of multiple internal states [27,45,46], or alternatively nonlinear readout protocols to exploit the correlated noise [47]. We verify that our protocol is robust to typical sources of decoherence in cavity-QED realizations and thus can be immediately relevant for state-of-the-art time and frequency standards.

Engineered FWM.—We consider an ensemble of atoms trapped by a deep one-dimensional magic optical lattice within an optical cavity, such that the spatial dynamics are effectively frozen. A single cavity mode, with angular frequency ω_c and power decay linewidth κ, couples to a long-lived optical transition, with angular frequency ω_a and natural decay rate $\gamma \ll \kappa$, between a manifold of ground (g) and excited (e) states with single-photon Rabi frequency $2g_0$ [see Fig. 1(a)]. We focus on the far-detuned limit, $|\Delta| = |\omega_c - \omega_a| \gg g_0\sqrt{N}, \kappa$, for N atoms, where the dynamics is near unitary. The cavity field can be adiabatically eliminated and serves only to mediate effective interactions between the atoms [48]. For concreteness of the following, we consider a system based on the Zeeman levels of the ${}^1\mathrm{S}_0$ (g) and ${}^3\mathrm{P}_0$ (e) electronic states in ${}^{87}\mathrm{Sr}$ with $F = 9/2$, which are separated by an optical transition frequency forming the basis of state-of-the-art optical lattice clocks [49]. However, our discussion can be generalized to alternative implementations using, e.g., spatially divided ensembles to emulate the multiple internal transitions [44,50].

We assume the atomic ensemble is prepared with an equal population of atoms in the electronic states $|g, m = -9/2\rangle$ and $|e, m = 9/2\rangle$, where m labels the spin projection of the Zeeman sublevel along the quantization axis set to be perpendicular to the cavity axis (e.g., by an external magnetic field). This initial state can be prepared using a combination of optical pumping and state-resolved transitions, as explained in [51]. Therein [see also Fig. 1(b)], we also verify that under this initial condition, the full atomic spin Hamiltonian involving all 20 levels in ${}^{87}\mathrm{Sr}$ dominantly drives cavity-mediated dynamics only in the quartet of states, $|g, m = \pm 9/2\rangle$ and $|e, m = \pm 9/2\rangle$, as the population of other Zeeman sublevels is suppressed by a combination of collective effects and favorable Clebsch-Gordan coefficients [51,55]. The atomic evolution is then described by the effective spin Hamiltonian [48,51],

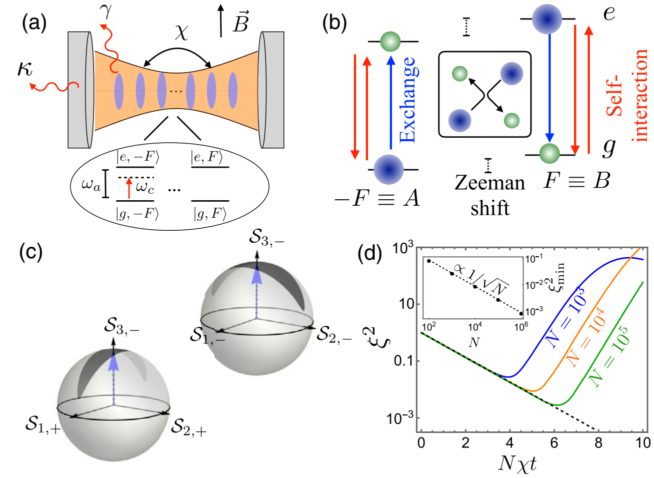

FIG. 1. (a) Schematic of cavity implementation: interactions (χ) between multilevel atoms (internal structure shown in inset) are mediated by exchange of virtual photons through a common cavity mode of angular frequency $\omega_c = \omega_a + \Delta$ where Δ is the detuning and ω_a is the atomic transition angular frequency. The cavity leaks photons through the mirrors at rate κ and the atoms undergo spontaneous emission at rate γ. A magnetic field perpendicular to the cavity axis provides a Zeeman shift, and sets the quantization direction. (b) Possible exchange processes (blue) and self-interactions (red) caused by cavity-mediated interactions. (c) Visualization of the spin squeezing generated during the dynamics, in the combined basis of the A and B manifolds. Blue arrows label the Bloch vector. (d) Squeezing, quantified by the normalized variance $\xi^2 = (4/N)(\Delta\mathcal{S}_{1,-})^2 = (4/N)(\Delta\mathcal{S}_{2,+})^2$, for $\delta = N\chi/2$ and different atom numbers N. The UPA prediction (dashed line) agrees with TWA calculations (solid lines) until corrections beyond UPA become important (see text). The minimum squeezing is $\xi^2_{\min} \approx 0.88/\sqrt{N}$ as shown in the inset.

$$\hat{H} = \hbar\chi\left(\hat{S}_A^+ + \hat{S}_B^+\right)\left(\hat{S}_A^- + \hat{S}_B^-\right) + \hbar\delta\left(\hat{S}_B^z - \hat{S}_A^z\right). \quad (1)$$

Hereafter, we denote the $m = -9/2(9/2)$ manifold as the $A(B)$ ensemble. We have introduced collective operators $\hat{S}_A^+ = \sum_{i=1}^N |e,A\rangle_i\langle g,A|_i$, $\hat{S}_B^+ = -\sum_i |e,B\rangle_i\langle g,B|_i$, and $\hat{S}_\alpha^z = 1/2\sum_i (|e,\alpha\rangle_i\langle e,\alpha|_i - |g,\alpha\rangle_i\langle g,\alpha|_i)$ for $\alpha = A$, B, where the summation runs over all N atoms. The sign convention for the B ensemble accounts for the differing sign of Clebsch-Gordan coefficients for the relevant transitions in each ensemble, which we absorb in the raising and lowering operators rather than Hamiltonian definition for convenience. The cavity detuning Δ controls the strength of the interaction, $\chi \approx -g_F^2/\Delta$ where the adjusted Rabi frequency $2g_F = 2g_0\sqrt{F/(F+1)}$ includes an additional factor $\sqrt{F/(F+1)}$ arising from Clebsch-Gordan coefficients [51]. A relative Zeeman shift, $\propto \delta$, splits the energies of the two ensembles.

The first term of Eq. (1) is a flip-flop process that includes (i) an exchange of an excitation between the A and

B ensembles, e.g., $\hat{S}_A^+\hat{S}_B^- + \mathrm{H.c.}$, and (ii) a self-interaction $\hat{S}_A^+\hat{S}_A^- + \hat{S}_B^+\hat{S}_B^-$. Both can be understood as the simultaneous destruction of a pair of particles in two atomic levels and subsequent creation of a pair in two levels, which is analogous to the process of FWM familiar from quantum and atom optics. We rigorize this analogy by defining Schwinger boson operators $\hat{a}_{g,\alpha}$ and $\hat{a}_{e,\alpha}$ via $\hat{S}_\alpha^+ = \hat{a}_{e,\alpha}^\dagger \hat{a}_{g,\alpha}$ to rewrite the spin Hamiltonian as

$$\hat{H}_{\mathrm{FWM}} = \hbar\chi\left(\hat{a}_{e,A}^\dagger\hat{a}_{g,A} + \hat{a}_{e,B}^\dagger\hat{a}_{g,B}\right)\left(\hat{a}_{g,A}^\dagger\hat{a}_{e,A} + \hat{a}_{g,B}^\dagger\hat{a}_{e,B}\right) + \frac{\hbar\delta}{2}\left(\hat{a}_{g,A}^\dagger\hat{a}_{g,A} + \hat{a}_{e,B}^\dagger\hat{a}_{e,B} - \hat{a}_{e,A}^\dagger\hat{a}_{e,A} - \hat{a}_{g,B}^\dagger\hat{a}_{g,B}\right), \tag{2}$$

where the first line describes a set of FWM processes. The Hamiltonian (2) is closely related to that realized via spin-changing interactions in spin-1 BECs [51] under the assumption that all atoms are restricted to a single common spatial mode. This assumption is not required in cavity-QED implementations [43,44,48] wherein the infinite-range interactions are generated by a uniform atomic coupling to a single common cavity mode, achieved by selective loading of the atoms in the spatial lattice or by adopting a ring cavity configuration.

Dynamics of pair creation.—In quantum optics it is common to make an undepleted pump approximation (UPA) [56] to study FWM, corresponding to replacing $\hat{a}_{g,A}, \hat{a}_{e,B} \sim \sqrt{N/2}$ in $\hat{H}_{\mathrm{FWM}}$. For simplicity, we have assumed that the two pump modes are equally populated and treat the general case with unequal pump populations in [51]. Further assuming $\delta = N\chi/2$ to effectively remove the mean-field interaction shift due to the self-interaction terms $\chi(\hat{S}_A^+\hat{S}_A^- + \hat{S}_B^+\hat{S}_B^-)$ [51] we obtain

$$\hat{H}_{\mathrm{TMS}} = \frac{N\hbar\chi}{2}\left(\hat{a}_{e,A}^\dagger\hat{a}_{g,B}^\dagger + \mathrm{H.c.}\right). \tag{3}$$

This final form elucidates a resonant production of pairs of bosons, or equivalently the correlated transfer of atom pairs to the internal levels $|e,A\rangle$ and $|g,B\rangle$. Using $\hat{H}_{\mathrm{TMS}}$, the number of entangled particles is $\bar{n}(t) = \langle\hat{a}_{e,A}^\dagger\hat{a}_{e,A} + \hat{a}_{g,B}^\dagger\hat{a}_{g,B}\rangle = 2\sinh^2(N\chi t/2)$ [32,57]. We benchmark the pair production and other predictions by Eq. (3) against the exact dynamics produced by Eq. (1) in [51].

Two-mode squeezing for enhanced metrology with an optical transition.—It is well established in quantum optics that the Hamiltonian Eq. (3) generates squeezing of combined two-mode quadrature fluctuations [58]. Considering $\chi > 0$ without loss of generality, within the UPA $\hat{H}$ produces squeezing along two bosonic quadratures labeled Y_+ and X_- and antisqueezing along conjugate quadratures X_+ and Y_- [51], with exponentially fast suppression or growth of the associated quantum noise $(\Delta X_\pm)^2 = \frac{1}{2}e^{\pm N\chi t}$ and $(\Delta Y_\pm)^2 = \frac{1}{2}e^{\mp N\chi t}$. In our proposal, the two-mode quadrature squeezing can be observed in collective spin operators that act on our four-level system. Specifically, the squeezed quadratures can be directly mapped to a combination of spin operators, $\sqrt{(N/2)}\hat{X}_- = \hat{\mathcal{S}}_{1,-} \equiv \hat{S}_B^x - \hat{S}_A^y$ and $\sqrt{(N/2)}\hat{Y}_+ = \hat{\mathcal{S}}_{2,+} \equiv \hat{S}_B^y + \hat{S}_A^x$. Correspondingly, the antisqueezed quadratures are $\sqrt{(N/2)}\hat{Y}_- = \hat{\mathcal{S}}_{2,-} \equiv \hat{S}_B^y - \hat{S}_A^x$ and $\sqrt{(N/2)}\hat{X}_+ = \hat{\mathcal{S}}_{1,+} \equiv \hat{S}_B^x + \hat{S}_A^y$.

We can visualize the squeezed quantum noise of the combined spin state corresponding to the A and B transitions on a pair of coupled Bloch spheres defined by axes $(\mathcal{S}_{1,-}, \mathcal{S}_{2,-}, \mathcal{S}_{3,-})$ and $(\mathcal{S}_{1,+}, \mathcal{S}_{2,+}, \mathcal{S}_{3,-})$ that share a common vertical component $\mathcal{S}_{3,-} = S_B^z - S_A^z$ and for which the corresponding operators obey standard SU(2) commutation relations [51]. As shown in Fig. 1(c), the state is squeezed in both Bloch spheres, $(\Delta\mathcal{S}_{1,-})^2 = (\Delta\mathcal{S}_{2,+})^2 = Ne^{-N\chi t}/4$, relative to the level of the initial separable state.

The UPA prediction for the squeezing, $(\Delta\mathcal{S}_{1,-})^2$ and $(\Delta\mathcal{S}_{2,+})^2$, is verified in Fig. 1(d) by comparing to a calculation of the variances based on a numerical simulation of the full multilevel cavity implementation, and we find excellent agreement up to $\bar{n} \sim 0.76\sqrt{N}$. The multilevel cavity dynamics are obtained using a truncated Wigner approximation (TWA), which approximates the quantum dynamics by averaging over an ensemble of classical trajectories with initial conditions chosen to reproduce the quantum fluctuations of the initial state [59–63]. We include all possible exchange processes between the complete set of $4F + 2$ ground and excited atomic levels in our TWA simulation, including, e.g., those mediated by photons with polarization perpendicular to the quantization axis [51,64].

A Ramsey protocol [65] that uses only collective rotations and population measurements of the spins encoded in the A and B manifolds can be used to take advantage of the squeezing in the Bloch sphere for enhanced sensing of phase shifts imprinted on the optical transition. The protocol is analogous to optical homodyne techniques in quantum optics, as well as atomic homodyne [45,66] or measurements of squeezing in spin-1 BECs [46,67]. However, as our atomic realization is based on four internal levels, as opposed to three in spin-1 BECs, we do not require any coherent mixing of the $F = \pm 9/2$ manifolds. This also distinguishes our approach from prior demonstrations of interferometry with Dicke-like states realized in spin-1 BECs [28], which treat the $m_F = \pm 1$ modes as the two internal levels of a collective spin-1/2 system and uses a Holland-Burnett-type protocol [68]. Such an approach is sensitive to decoherence [69] and readout errors [19], while in our system it would also add the complex requirement of engineering a coupling between the $F = \pm 9/2$ states.

Here, we present Ramsey protocols for measuring sum and difference optical phases imprinted on the atoms, illustrated in Fig. 2. Measuring differential phases has several applications including gravimetry [70], measuring gravitational redshifts [71–74], and detecting gravitational waves [75,76] and dark matter [77]. Measuring the sum phase is useful for improving state-of-the-art optical atomic clocks.

To measure a differential phase imprinted by a rotation about $S_B^z - S_A^z$, we begin our protocol with a $\pi/2$ pulse that rotates atoms in the A ensemble about S^x and those in the B ensemble by S^y, i.e., implements $\exp[-i(\pi/2)\hat{\mathcal{S}}_{2,+}]$. Next, we accumulate a relative phase shift by a rotation of ϕ about $-S_A^z$ and S_B^z (i.e., $\mathcal{S}_{3,-}$), and finally apply a second $\pi/2$ pulse which rotates atoms in the A and B ensembles about S^y and S^x, i.e., implements $\exp[-i(\pi/2)\hat{\mathcal{S}}_{1,+}]$. The action of this pulse sequence on the state is best visualized by looking at the spin distribution on the Bloch spheres, as shown in Fig. 2(a), where the initial spin distribution is to that of the lower Bloch sphere in Fig. 1(c). The final pulse converts the rotation $\hat{U}_\phi$ into a change in the difference in atomic inversions

$$\langle \hat{S}_B^z - \hat{S}_A^z \rangle = \frac{N}{2}\sin\phi. \tag{4}$$

This Ramsey sequence does not imprint any information about the differential phase on the upper Bloch sphere in Fig. 1(c) [51].

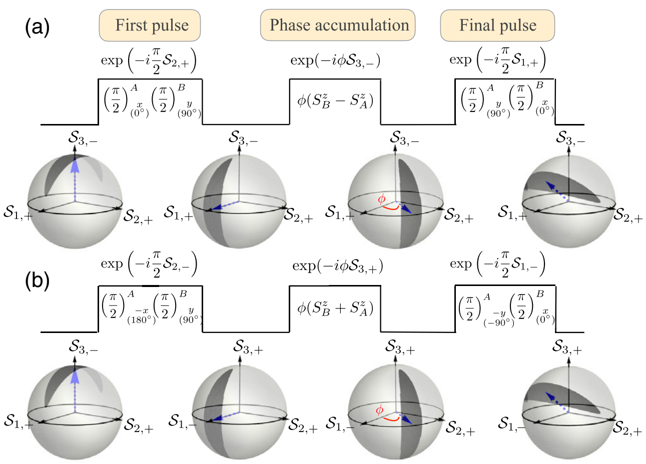

FIG. 2. (a) Ramsey sequence to measure a differential clock phase shift imprinted on the atoms. A first $\pi/2$ pulse rotates the Bloch vector to the equator. Next, a phase accumulation rotates the Bloch vector about $S_B^z - S_A^z$ by an angle ϕ, before a final $\pi/2$ pulse rotates the Bloch vector for readout via measuring $\hat{S}_B^z - \hat{S}_A^z$. (b) Ramsey sequence to measure the sum phase imprinted on the atoms. The first $\pi/2$ pulse defines the squeezed distribution on a joint Bloch sphere of A and B defined by the axes $(\mathcal{S}_{1,-}, \mathcal{S}_{2,+}, \mathcal{S}_{3,+})$. After phase accumulation about $S_B^z + S_A^z$, the final pulse again rotates the Bloch vector for readout via measuring $\hat{S}_B^z + \hat{S}_A^z$. In both cases, dashed blue arrows mark the Bloch vector at each stage. The subscript $x(y)$ for the pulses denote the axis of rotation $S_x(S_y)$, and the degree $0^\circ(90^\circ)$ in the subscript conveys the same information via the phase of the laser pulse.

The sum phase, imprinted by a collective rotation around $\mathcal{S}_{3,+} \equiv S_A^z + S_B^z$, is similarly inferred by another Ramsey protocol shown in Fig. 2(b). Note that neither Bloch sphere in Fig. 1(c) has $\mathcal{S}_{3,+}$ as an axis. Therefore, the first pulse in this Ramsey protocol, implementing $\exp[-i(\pi/2)\hat{\mathcal{S}}_{2,-}]$, is chosen such that it rotates the axes in the Bloch sphere from $(\mathcal{S}_{1,+}, \mathcal{S}_{2,+}, \mathcal{S}_{3,-})$ to $(-\mathcal{S}_{3,+}, \mathcal{S}_{2,+}, \mathcal{S}_{1,-})$, thus introducing $\mathcal{S}_{3,+}$ into relevance. The remainder of the sequence proceeds analogously to that for the differential phase.

The sensitivity of both protocols, computed within the UPA, is

$$(\Delta\phi)^2 \equiv \frac{(\Delta O)^2}{(d\langle\hat{O}\rangle/d\phi)^2} = \frac{e^{-N\chi t}}{N} + \frac{\bar{n}(\bar{n}+2)}{4N^2}\tan^2\phi, \tag{5}$$

where $\hat{O}$ is the observable measured. Equation (5) predicts an advantage relative to the standard quantum limit (SQL), $(\Delta\phi)^2 = 1/N$, which sets the optimal resolution achievable with uncorrelated particles, for any $\bar{n} > 0$ and a wide dynamic range of ϕ, $|\tan\phi| < 2\sqrt{N}/\bar{n}$, which can be $\mathcal{O}(1)$.

The sensitivity [Eq. (5)] can be degraded by other effects not included in the ideal analysis, including (i) corrections beyond the UPA, (ii) decoherence, and (iii) fluctuations in the total and relative populations of the A and B ensembles. We discuss (i) and (ii) below, and leave the discussion on (iii) to [51]. There, we show that number fluctuations at the level of shot noise provide a comparable degradation of the sensitivity to that generated by (i) and (ii).

The leading corrections to $\hat{H}_{\mathrm{TMS}}$ can be captured by iteratively modifying the UPA to include depletion of the pump states $|g, A\rangle$ and $|e, B\rangle$ by $\bar{n}/2$. This is achieved by setting $\hat{a}_{g,A}, \hat{a}_{e,B} \approx \sqrt{[(N-\bar{n})/2]}$ where $\bar{n} = 2\sinh^2(N\chi t/2)$ is taken to be the original UPA result as a first approximation. Making this correction has two physical consequences [51]: (i) the effective nonlinearity $\chi(N-\bar{n})/2$ driving pair production is reduced relative to the UPA, and (ii) the pair production is no longer resonant as the Zeeman shift $\delta = \chi N/2$ is static and does not completely cancel the mean-field shift introduced by the self-interaction terms in Eq. (2). For $1 \ll \bar{n} \ll N$ we then obtain the beyond-UPA sensitivity [51]

$$(\Delta\phi)^2 \approx \frac{1}{2N\bar{n}} + \frac{\bar{n}^3}{2N^3} + \frac{\bar{n}(\bar{n}+2)}{4N^2}\tan^2\phi. \tag{6}$$

The optimal sensitivity remains enhanced relative to the SQL, with a lower bound of $(\Delta\phi)^2 = 2/(3^{3/4}N^{3/2})$ that occurs for $\bar{n} = \sqrt{N}/3^{1/4}$, in agreement with TWA results.

Decoherence.—Dissipative noise in our system intrinsically arises from superradiant decay, at a rate $\Gamma \approx g_F^2\kappa/\Delta^2$, due to leakage of the photons that mediate the effective atom-atom interaction from the cavity, and single particle spontaneous emission into free space at the rate γ. While both are deleterious for sensing, we show that our protocol

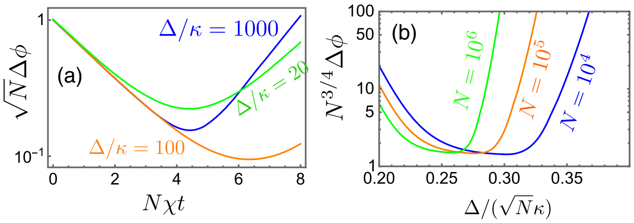

FIG. 3. (a) Scaled sensitivity $\sqrt{N}\Delta\phi$ versus time for different cavity detunings Δ, and $C = 10$ and $N = 10^5$. The best sensitivity is achieved at an optimum time for each Δ. (b) Scaled best sensitivity $N^{3/4}\Delta\phi$ versus $\Delta/(\sqrt{N}\kappa)$. In each case, the minima occur at similar $\Delta/(\sqrt{N}\kappa)$, and have similar values (up to logarithmic corrections).

can achieve sub-SQL sensitivity even with these sources of decoherence.

Collective decay is treated by solving a Lindblad master equation with jump operator $\hat{L} = \sqrt{\Gamma}(\hat{S}_A^- + \hat{S}_B^-)$, which captures the dominant process where an emitted photon polarized along the quantization axis is lost from the cavity [51]. Spontaneous emission is included through jump operators $\hat{L}_i = \sqrt{\gamma}(\hat{\sigma}_{A,i}^- + \hat{\sigma}_{B,i}^-)$, where $\sigma_{\alpha,i}^-$ is the spin-lowering operator in the $\alpha = A, B$ manifold for the ith atom.

In Fig. 3(a) we plot the scaled sensitivity $\sqrt{N}\Delta\phi$ as a function of time in the presence of decoherence for a range of cavity detunings. It decreases from the initial SQL to a minimum value at an optimum time that depends on the detuning. This optimum time balances the gain obtained by reaching a higher $\bar{n}$ versus the loss in squeezing due to decoherence. Optimizing this interplay via Δ (thus tuning χ relative to Γ and γ), we obtain a best achievable sensitivity [see Fig. 3(b) and [51]]

$$(\Delta\phi)^2 = \frac{\sqrt{2\ln(2NC)}}{N^{3/2}\sqrt{C}}, \tag{7}$$

for $\Delta = [\kappa\sqrt{NC}/2\sqrt{\ln(2NC)}]$, with $C = 4g_F^2/\kappa\gamma$ the single-atom cooperativity. Current experimental setups [43,55], with $\kappa/2\pi \sim 150$ kHz and $g/2\pi \sim 4$ Hz, can reach a collective cooperativity $NC = 4 \times 10^5$ with $N = 10^6$ atoms, and $NC = 10^7$ is within reach. The sensitivity in Eq. (7) is only slightly degraded from the ideal case [see Fig. 1(d) and Eq. (6)] and is competitive with the best sensitivities achievable with the paradigmatic approach of one-axis twisting when decoherence is incorporated [1,13,78].

Outlook.—Our proposal offers new opportunities to study and exploit the exponentially rapid generation of entanglement in atomic systems, driven by connections to well established concepts in quantum optics. Moreover, our proposal highlights new possibilities for the realization and investigation of diverse models of bosonic pair production in highly tunable quantum simulators featuring spin-spin interactions.

We thank M. Affolter, A. Carter, and T. Bilitewski for a careful reading and comments on the manuscript. A. M. R. acknowledges support from the Air Force Office of Scientific Research Grants No. FA9550-18-1-0319 and No. FA9550-19-1-0275, from the Defense Advanced Research Projects Agency and Army Research Office Grant No. W911NF-16-1-0576, by the National Science Foundation JILA-Physics Frontier Center Grant No. PHY-1734006, Quantum Leap Challenge Institute—Office of Multidisciplinary Activities Grant No. 2016244, by the U.S. Department of Energy, Office of Science, National Quantum Information Science Research Centers Quantum Systems Accelerator, and from the National Institute of Standards and Technology. R. L. S. acknowledges support from the National Science Foundation Grant No. PHY-2110052.

[1] A. Chu, P. He, J. K. Thompson, and A. M. Rey, Phys. Rev. Lett. **127**, 210401 (2021).
[2] Z. Ahmed, Y. Alexeev, G. Apollinari, A. Arvanitaki, D. Awschalom, K. K. Berggren, K. Van Bibber, P. Bienias, G. Bodwin, M. Boshier *et al.*, arXiv:1803.11306.
[3] K. M. Backes, D. A. Palken, S. Al Kenany, B. M. Brubaker, S. B. Cahn, A. Droster, G. C. Hilton, S. Ghosh, H. Jackson, S. K. Lamoreaux *et al.*, Nature (London) **590**, 238 (2021).
[4] A. Arvanitaki, J. Huang, and K. Van Tilburg, Phys. Rev. D **91**, 015015 (2015).
[5] A. Derevianko and M. Pospelov, Nat. Phys. **10**, 933 (2014).
[6] S. Kolkowitz, I. Pikovski, N. Langellier, M. D. Lukin, R. L. Walsworth, and J. Ye, Phys. Rev. D **94**, 124043 (2016).
[7] R. M. Godun, P. B. R. Nisbet-Jones, J. M. Jones, S. A. King, L. A. M. Johnson, H. S. Margolis, K. Szymaniec, S. N. Lea, K. Bongs, and P. Gill, Phys. Rev. Lett. **113**, 210801 (2014).
[8] C. Sanner, N. Huntemann, R. Lange, C. Tamm, E. Peik, M. S. Safronova, and S. G. Porsev, Nature (London) **567**, 204 (2019).
[9] B. M. Roberts, P. Delva, A. Al-Masoudi, A. Amy-Klein, C. Baerentsen, C. F. A. Baynham, E. Benkler, S. Bilicki, S. Bize, W. Bowden *et al.*, New J. Phys. **22**, 093010 (2020).
[10] E. Pedrozo-Peñafiel, S. Colombo, C. Shu, A. F. Adiyatullin, Z. Li, E. Mendez, B. Braverman, A. Kawasaki, D. Akamatsu, Y. Xiao, and V. Vuletić, Nature (London) **588**, 414 (2020).
[11] I. D. Leroux, M. H. Schleier-Smith, and V. Vuletić, Phys. Rev. Lett. **104**, 250801 (2010).
[12] J. Hu, L. Feng, Z. Zhang, and C. Chin, Nat. Phys. **15**, 785 (2019).
[13] R. J. Lewis-Swan, M. A. Norcia, J. R. K. Cline, J. K. Thompson, and A. M. Rey, Phys. Rev. Lett. **121**, 070403 (2018).
[14] Y.-C. Zhang, X.-F. Zhou, X. Zhou, G.-C. Guo, and Z.-W. Zhou, Phys. Rev. Lett. **118**, 083604 (2017).
[15] R. J. Lewis-Swan, D. Barberena, J. A. Muniz, J. R. K. Cline, D. Young, J. K. Thompson, and A. M. Rey, Phys. Rev. Lett. **124**, 193602 (2020).
[16] S. J. Masson, M. D. Barrett, and S. Parkins, Phys. Rev. Lett. **119**, 213601 (2017).

[17] E. Davis, G. Bentsen, and M. Schleier-Smith, Phys. Rev. Lett. **116**, 053601 (2016).

[18] E. Davis, G. Bentsen, T. Li, and M. Schleier-Smith, in *Advances in Photonics of Quantum Computing, Memory, and Communication X* (International Society for Optics and Photonics, San Fransisco, CA, 2017), Vol. 10118, p. 101180Z.

[19] Q. Guan, G. W. Biedermann, A. Schwettmann, and R. J. Lewis-Swan, Phys. Rev. A **104**, 042415 (2021).

[20] G. S. Agarwal, *Quantum Optics* (Cambridge University Press, Cambridge, England, 2012).

[21] R. Bücker, J. Grond, S. Manz, T. Berrada, T. Betz, C. Koller, U. Hohenester, T. Schumm, A. Perrin, and J. Schmiedmayer, Nat. Phys. **7**, 608 (2011).

[22] M. Bonneau, J. Ruaudel, R. Lopes, J.-C. Jaskula, A. Aspect, D. Boiron, and C. I. Westbrook, Phys. Rev. A **87**, 061603(R) (2013).

[23] Y.-Q. Zou, L.-N. Wu, Q. Liu, X.-Y. Luo, S.-F. Guo, J.-H. Cao, M. K. Tey, and L. You, Proc. Natl. Acad. Sci. U.S.A. **115**, 6381 (2018).

[24] S. S. Hodgman, R. I. Khakimov, R. J. Lewis-Swan, A. G. Truscott, and K. V. Kheruntsyan, Phys. Rev. Lett. **118**, 240402 (2017).

[25] J.-C. Jaskula, M. Bonneau, G. B. Partridge, V. Krachmalnicoff, P. Deuar, K. V. Kheruntsyan, A. Aspect, D. Boiron, and C. I. Westbrook, Phys. Rev. Lett. **105**, 190402 (2010).

[26] F. Borselli, M. Maiwöger, T. Zhang, P. Haslinger, V. Mukherjee, A. Negretti, S. Montangero, T. Calarco, I. Mazets, M. Bonneau, and J. Schmiedmayer, Phys. Rev. Lett. **126**, 083603 (2021).

[27] C. Gross, H. Strobel, E. Nicklas, T. Zibold, N. Bar-Gill, G. Kurizki, and M. K. Oberthaler, Nature (London) **480**, 219 (2011).

[28] B. Lücke, M. Scherer, J. Kruse, L. Pezzé, F. Deuretzbacher, P. Hyllus, J. Peise, W. Ertmer, J. Arlt, L. Santos, A. Smerzi, and C. Klempt, Science **334**, 773 (2011).

[29] E. M. Bookjans, C. D. Hamley, and M. S. Chapman, Phys. Rev. Lett. **107**, 210406 (2011).

[30] A. T. Black, E. Gomez, L. D. Turner, S. Jung, and P. D. Lett, Phys. Rev. Lett. **99**, 070403 (2007).

[31] L. Zhao, J. Jiang, T. Tang, M. Webb, and Y. Liu, Phys. Rev. A **89**, 023608 (2014).

[32] A. Qu, B. Evrard, J. Dalibard, and F. Gerbier, Phys. Rev. Lett. **125**, 033401 (2020).

[33] K. Kim, J. Hur, S. J. Huh, S. Choi, and J.-y. Choi, Phys. Rev. Lett. **127**, 043401 (2021).

[34] E. S. Polzik and J. Ye, Phys. Rev. A **93**, 021404(R) (2016).

[35] G. Vasilakis, H. Shen, K. Jensen, M. Balabas, D. Salart, B. Chen, and E. S. Polzik, Nat. Phys. **11**, 389 (2015).

[36] J. Appel, P. J. Windpassinger, D. Oblak, U. B. Hoff, N. Kjærgaard, and E. S. Polzik, Proc. Natl. Acad. Sci. U.S.A. **106**, 10960 (2009).

[37] M. H. Schleier-Smith, I. D. Leroux, and V. Vuletić, Phys. Rev. Lett. **104**, 073604 (2010).

[38] J. G. Bohnet, K. C. Cox, M. A. Norcia, J. M. Weiner, Z. Chen, and J. K. Thompson, Nat. Photonics **8**, 731 (2014).

[39] R. J. Sewell, M. Koschorreck, M. Napolitano, B. Dubost, N. Behbood, and M. W. Mitchell, Phys. Rev. Lett. **109**, 253605 (2012).

[40] H. Bao, J. Duan, S. Jin, X. Lu, P. Li, W. Qu, M. Wang, I. Novikova, E. E. Mikhailov, K.-F. Zhao *et al.*, Nature (London) **581**, 159 (2020).

[41] C. K. Law, H. Pu, and N. P. Bigelow, Phys. Rev. Lett. **81**, 5257 (1998).

[42] J. Jie, Q. Guan, S. Zhong, A. Schwettmann, and D. Blume, Phys. Rev. A **102**, 023324 (2020).

[43] M. A. Norcia, R. J. Lewis-Swan, J. R. K. Cline, B. Zhu, A. M. Rey, and J. K. Thompson, Science **361**, 259 (2018).

[44] E. J. Davis, G. Bentsen, L. Homeier, T. Li, and M. H. Schleier-Smith, Phys. Rev. Lett. **122**, 010405 (2019).

[45] J. Peise, I. Kruse, K. Lange, B. Lücke, L. Pezzè, J. Arlt, W. Ertmer, K. Hammerer, L. Santos, A. Smerzi, and C. Klempt, Nat. Commun. **6**, 8984 (2015).

[46] C. D. Hamley, C. S. Gerving, T. M. Hoang, E. M. Bookjans, and M. S. Chapman, Nat. Phys. **8**, 305 (2012).

[47] D. Linnemann, H. Strobel, W. Muessel, J. Schulz, R. J. Lewis-Swan, K. V. Kheruntsyan, and M. K. Oberthaler, Phys. Rev. Lett. **117**, 013001 (2016).

[48] J. A. Muniz, D. Barberena, R. J. Lewis-Swan, D. J. Young, J. R. K. Cline, A. M. Rey, and J. K. Thompson, Nature (London) **580**, 602 (2020).

[49] A. D. Ludlow, M. M. Boyd, J. Ye, E. Peik, and P. O. Schmidt, Rev. Mod. Phys. **87**, 637 (2015).

[50] A. Periwal, E. S. Cooper, P. Kunkel, J. F. Wienand, E. J. Davis, and M. Schleier-Smith, Nature (London) **600**, 630 (2021).

[51] See Supplemental Material at http://link.aps.org/supplemental/10.1103/PhysRevLett.130.113202 which includes Refs. [19,20,41–43,48,52–54], for derivations of master equation, squeezing, higher-order corrections, and numerical benchmarks.

[52] M. A. Norcia, J. R. Cline, J. A. Muniz, J. M. Robinson, R. B. Hutson, A. Goban, G. E. Marti, J. Ye, and J. K. Thompson, Phys. Rev. X **8**, 021036 (2018).

[53] M. M. Boyd, T. Zelevinsky, A. D. Ludlow, S. M. Foreman, S. Blatt, T. Ido, and J. Ye, Science **314**, 1430 (2006).

[54] A. Polkovnikov, Ann. Phys. (Amsterdam) **325**, 1790 (2010).

[55] M. A. Norcia, M. N. Winchester, J. R. K. Cline, and J. K. Thompson, Sci. Adv. **2**, e1601231 (2016).

[56] C. Gerry and P. Knight, Nonclassical light, in *Introductory Quantum Optics* (Cambridge University Press, Cambridge, England, 2004), pp. 150–194.

[57] A. I. Lvovsky, Photonics **1**, 121 (2015).

[58] D. F. Walls and G. J. Milburn, *Quantum Optics*, 2nd ed. (Springer, New York, 2008).

[59] B. Zhu, A. M. Rey, and J. Schachenmayer, New J. Phys. **21**, 082001 (2019).

[60] S. Lepoutre, J. Schachenmayer, L. Gabardos, B. Zhu, B. Naylor, E. Maréchal, O. Gorceix, A. M. Rey, L. Vernac, and B. Laburthe-Tolra, Nat. Commun. **10**, 1714 (2019).

[61] J. Schachenmayer, A. Pikovski, and A. M. Rey, Phys. Rev. X **5**, 011022 (2015).

[62] A. Patscheider, B. Zhu, L. Chomaz, D. Petter, S. Baier, A.-M. Rey, F. Ferlaino, and M. J. Mark, Phys. Rev. Res. **2**, 023050 (2020).

[63] B. Sundar, K. C. Wang, and K. R. A. Hazzard, Phys. Rev. A **99**, 043627 (2019).

[64] A. Piñeiro Orioli, J. K. Thompson, and A. M. Rey, Phys. Rev. X **12**, 011054 (2022).

[65] J. Ma, X. Wang, C.-P. Sun, and F. Nori, Phys. Rep. **509**, 89 (2011).

[66] W. Muessel, H. Strobel, D. Linnemann, D. B. Hume, and M. K. Oberthaler, Phys. Rev. Lett. **113**, 103004 (2014).

[67] F. Anders, L. Pezzè, A. Smerzi, and C. Klempt, Phys. Rev. A **97**, 043813 (2018).

[68] M. J. Holland and K. Burnett, Phys. Rev. Lett. **71**, 1355 (1993).

[69] S. F. Huelga, C. Macchiavello, T. Pellizzari, A. K. Ekert, M. B. Plenio, and J. I. Cirac, Phys. Rev. Lett. **79**, 3865 (1997).

[70] G. M. Tino, Quantum Sci. Technol. **6**, 024014 (2021).

[71] T. Bothwell, C. J. Kennedy, A. Aeppli, D. Kedar, J. M. Robinson, E. Oelker, A. Staron, and J. Ye, Nature (London) **602**, 420 (2022).

[72] C.-W. Chou, D. B. Hume, T. Rosenband, and D. J. Wineland, Science **329**, 1630 (2010).

[73] J. Grotti, S. Koller, S. Vogt, S. Häfner, U. Sterr, C. Lisdat, H. Denker, C. Voigt, L. Timmen, A. Rolland *et al.*, Nat. Phys. **14**, 437 (2018).

[74] M. Takamoto, I. Ushijima, N. Ohmae, T. Yahagi, K. Kokado, H. Shinkai, and H. Katori, Nat. Photonics **14**, 411 (2020).

[75] M. e. Tse, H. Yu, N. Kijbunchoo, A. Fernandez-Galiana, P. Dupej, L. Barsotti, C. D. Blair, D. D. Brown, S. E. Dwyer, A. Effler *et al.*, Phys. Rev. Lett. **123**, 231107 (2019).

[76] F. Acernese, M. Agathos, L. Aiello, A. Allocca, A. Amato, S. Ansoldi, S. Antier, M. Arène, N. Arnaud, S. Ascenzi *et al.*, Phys. Rev. Lett. **123**, 231108 (2019).

[77] C. J. Kennedy, E. Oelker, J. M. Robinson, T. Bothwell, D. Kedar, W. R. Milner, G. E. Marti, A. Derevianko, and J. Ye, Phys. Rev. Lett. **125**, 201302 (2020).

[78] J. Hu, W. Chen, Z. Vendeiro, A. Urvoy, B. Braverman, and V. Vuletić, Phys. Rev. A **96**, 050301(R) (2017).